UNIZIK JOURNAL OF ENGINEERING AND APPLIED SCIENCES (UJEAS)

Research Article

Watermelon Rind Extract as a Green Corrosion Inhibitor for Mild Steel in Acid media

Emembolu, L. N., Akpu, S. C., Ejiofor, C. C., Ajali J. J., Igbokwe P. K.

Special Issue
A Themed Issue in Honour of Professor Onukwuli Okechukwu Dominic (FAS).

This special issue is dedicated to Professor Onukwuli Okechukwu Dominic (FAS), marking his retirement and celebrating a remarkable career. His legacy of exemplary scholarship, mentorship, and commitment to advancing knowledge is commemorated in this collection of works.

Edited by
Chinonso Hubert Achebe PhD.
Christian Emeka Okafor PhD.

UJEAS

UNIZIK JOURNAL OF ENGINEERING AND APPLIED SCIENCES

UNIZIK Journal of Engineering and Applied Sciences 4(2), March (2025), 1945 - 1957
Journal homepage: https://journals.unizik.edu.ng/index.php/ujeas
PRINT ISSN: 2992-4383 || ONLINE ISSN: 2992-4391

Watermelon Rind Extract as a Green Corrosion Inhibitor for Mild Steel in Acid media

*,[1]Emembolu, L. N., [1]Akpu, S. C., [1]Ejiofor, C. C., [1]Ajali J. J., [1]Igbokwe P. K.

[1]Department of Chemical Engineering Nnamdi Azikiwe University, Awka.
* Corresponding Author's E-mail: ln.emembolu@unizik.edu.ng.

Abstract
In this work, the juice from watermelon rinds, known as watermelon rind extracts (WMRE), was extracted and employed as a potent corrosion inhibitor on mild- steel in 1 M HCl. An evaluation of WMRE's ability to reduce mild steel corrosion in 1 M HCl was conducted using gravimetric measurements. Fourier transform infrared (FTIR) spectroscopy was used to ascertain the chemical composition of WMRE, while GC-FID was used to investigate its phytochemical components. The scanning electron microscope (SEM and EDX) gave further information about the surface shape and configuration. The findings showed that an enhanced inhibition efficiency (from 50.32 to 88.41%) was attained by raising the inhibitor concentration (from 100 to 600 mg/l) at a modest operating temperature of 303 K. The organic functional groups responsible for the inhibitory activity were identified by the FTIR findings. Furthermore, GC-FID demonstrated that the mild steel was shielded from corrosive conditions by the active phytochemical components that were adsorbed on its surface and contained WMRE. The development of an adsorbed inhibitor protective layer on the steel surface was demonstrated by SEM and EDX analyses. Accordingly, the thermodynamic kinetic characteristics of WMRE adsorption on mild-steel surface sites follows the Frumkin > Langmuir > Temkin adsorption isotherm respectively.

Keywords: WMRE, mild-steel, Green inhibitor, GC-FID, EDX and SEM

1. Introduction

Corrosion damage impacts the reliability of industrial operations and materials distribution (Jun et al., 2018). In industries that deal on toxic chemicals, damages such as pipeline leaks results to adverse environmental and health complications**.** Studying mild steel corrosion is crucial for economical industrial operations since mild steel is the most commonly used engineering material because of its hardness, affordability, and ease of production (Askeland & Phule, 2016). One of the main limitations of mild steel's applications is its weak acid corrosion resistance Olivia et al. (2023), Okeoma et al (2022), and Priyotomo, et al in (2022). Its corrosion processes can be effectively and practically controlled by using inhibitors (Emembolu & Igwegbe, 2022; Anaele & Ipeghan 2018). Nevertheless, the majority of the substances that make up these inhibitors are harmful to both people and their surroundings. The toxicity of these inorganic and organic inhibitors has opened the door to investigating the use of ecologically benign, non-toxic natural product inhibitors (Norbaayah, etal, 2021**;** Onyenanu, et al, 2022; Lasisi et al 2023; Bhoomika, etal, (2024);.

Some plant extracts have been used to prevent steel from corroding in acidic environments [Lasisi et al (2023); Amine, et al (2023); Emembolu, etal, 2024; Bhoomika, etal, (2024); Norbaayah, etal, (2021**);** Barboza, et al, (2024); Alan Miralrio and Araceli Espinoza, (2020); Radha, et al, (2024); Singh, et al, (2025); Onyenanu, et al, (2022)]. A blooming plant that resembles a vine, watermelon is a member of the Cucurbitaceae family and comes in both seeded and seedless variants. Its huge edible fruits, which have a juicy reddish, yellowish, or pink pulp and a rigid green rind, are the reason it is planted so widely. It is a necessary agricultural product that is used to make a variety of food items, including fruit juices, nectars, and cocktails Anaele & Ipeghan; Emembolu, etal, 2024. The pulp of the watermelon is its most valuable component for the food business. Both fresh and dried watermelon peel, watermelon pulp and watermelon rind (WMR) contain significant amounts of anti-nutrients, including saponin,

alkaloids, hydrogen cyanide, tannins, phytate, phenol, oxalate, and flavonoids, according to Singh, et al, (2025). Furthermore, citrulline, a non-essential amino acid, has been found to naturally occur in WMR, an agricultural waste product Norbaayah, etal, (2021**)**. Fig. 1 depicts the chemical structure of citrulline, the main ingredient in WMRE. The extracts made from watermelon waste products may have promise as corrosion inhibitors since these chemicals contain heteroatoms (N, O) and aromatic rings, which are thought to be centers of adsorption. The application of watermelon pieces as a metal corrosion inhibitor in some harsh situations has not received much attention. For example, watermelon leaf and watermelon peel extract (WMPE) have been utilized to prevent zinc corrosion in natural seawater Alan Miralrio and Araceli Espinoza V., (2020). To the best of our knowledge, however, there is no report on the application of watermelon rind as a corrosion inhibitor for any metal in a corrosive environment.

Thus, using kinetics and thermodynamics trends across a range of WMRE dosages and temperatures, this work investigates the chemistry behind the inhibitory activity of WMRE in 1M HCl media. Active inhibitory agents of WMRE were found by a variety of microscopic and spectroscopic investigations, including FTIR, SEM, EDS, and GC-FID assays. Because of its biodegradability, which lessens negative environmental effects, watermelon rind extracts are effective and far superior to traditional inorganic materials.

2.0 Materials and methods

2.1 Sourcing and preparation of materials

2.1.1 Watermelon rind Extract (WMRE)

Watermelon rinds were sourced from a waste disposal site in the municipality of Ifite in Awka Nigeria. This was identified at the Department of Botany, Nnamdi Azikiwe University –Awka. They were cut into smaller chops and thoroughly washed (first with regular water to flush out sand and other debris, and then with distilled water). The dirt-free rinds were dried in the oven at 60°C, for 72 hours, ground and weighed. The extraction of WMRE was done according to procedures described previously in Emembolu, et al, (2021).

2.1.2 Mild-Steel coupons

The Mild-steel sheet utilized in this work was purchased locally from Eke Awka market. It was polished with an emery paper and degreased with acetone, as previously described in Emembolu, et al, 2021. The mild steel sheet was then carefully cut into 15 equal square samples, or coupons, each measuring 3 cm by 3 cm by 0.1 cm. They were then weighed and registered. Using 1 cm^2 as the working area, the mild-steel coupons were made up of 0.36 % C, 0.27 % Si, 0.66 % Mn, 0.02 % S, 0.21 % Cr, 0.015 % P, 0.06 % Al, 0.02 % Mo, and 0.22 % Cu, with the remainder being iron.

2.1.3 Test solution

In a 250 ml volumetric flask, precisely 88 ml of the stock solution of HCl (purity: 35%, specific gravity: 1.18), half-filled with water, and vigorously swirled. The solution was then topped off with more distilled water to reach the 250 ml flask mark. Before being used, this solution was kept out of direct sunlight.

2.2 Methods

2.2.1 Instrumental Characterizations

2.2.1.1 Gas Chromatography –Flame Ionization Detection (GC-FID)

A RESTEK 15 meter MXT-1 column (15 m x 250µm x 0.15µm) and a BUCK M910 gas chromatography with a flame ionization detector were utilized for the phytochemicals analysis.

2.2.2 Surface analysis (SEM/ EDX)

The surface morphology of the mild-steel samples was examined using energy-dispersive X-ray analysis (EDX) technology in combination with scanning electron microscopy (SEM). Mild steel coupons used in the surface morphology experiment were submerged in a 1 M HCl solution for 12 hours at 303–323K, both with and without varying WMRE concentrations.

2.2.3 FTIR analysis

The presence of several functional groups and aromatic groups in the WMRE was determined using FT-IR analysis. To create the sample pallet, concentrated WMRE and KBr were combined. A Shimadzu FTIR 8400S spectrophotometer operating at a frequency of 400–4000 cm-1 was used to analyze this material.

2.3 Weight loss study

Before drying, the mild-steel coupons were carefully cleaned with double-distilled water, weighed three times, and their average was recorded using an analytical balance. Next, each coupon was immersed in a 1 M HCl solution containing varying concentrations of WMRE for 0 to 10 hours at various temperatures (303 to 323K) to study the corrosion resistivity of WMRE. Each step was repeated twice to ensure the accuracy of the results obtained. After the above steps, weight loss analysis was used to determine the corrosion resistance of WMRE, the inhibitory actions of the WMRE were evaluated, and the degree of mild steel corrosion was assessed using the following equations: Emembolu et al., 2021; Mohamed, 2022).

$$C_R = \frac{W_1 - W_2}{A\,X} \quad (1)$$

$$IE(\%) = \frac{C_R^o - C_R^i}{C_R^o} X100 \quad (2)$$

$$\theta = \frac{C_R^o - C_R^i}{C_R^o} \quad (3)$$

Where

C_R = Corrosion rate

w_1 and w_2 = weight loss before and after being submerged in the testing solution, (mg)

t = immersion duration (hr)

A = area of coupon

θ = surface coverage

C_R^i = Corrosion rate with the inhibitor

C_R^0 = Corrosion rate without the inhibitor

IE = Inhibition efficiency in percent

3.0 Result and Discussion

3.1 Phytochemicals

The phytochemical contents of WMRE were detected and quantified using GC-FID due to its ease of use, sensitivity to organic chemicals, and improved quantitative accuracy especially in quantifying numerous components, particularly hydrocarbons.

Table 1: Phytochemical results on the WMRE via GC-FID

Components	Concentration(mg/ml)
Phenol	28.2678
Tanin	53.9739
Rutin	13.5726
Anthocyanin	10.9846
Lunamarine	9.6043
Oxalate	11.9510
Epicatechin	2.3499
Phytate	5.1254
Sapogenin	5.5409
Ribalinidine	7.8928
Saponin	22.4043
Catechin	3.9510
Kaempferol	15.5789

As can be seen from Table 1 above, WMRE has antioxidant components like Phenol, Bramatyo et al. (2024), Tannin, Mohammad et al. (2024), Rutin, Nikitia et al. (2023), Anthocyanin, Nnanna (2018), Saponin, and others.

These components are WMRE's primary anti-oxidative properties, which allow it to thwart the metal-oxygen electrochemical reaction and prevent corrosion.

3.2 Corrosion study

As indicated in Table 2, the mild-steel coupons' weight loss investigation was conducted to examine the corrosion inhibition effectiveness, corrosion rate, and surface coverage at different WMRE concentrations (0 to 600 mg/l).
Table 2 shows that the corrosion rate, corrosion inhibition efficiency, and surface coverage of the WMRE inhibitor increase with increasing concentration, peaking at the 600mg/l optimal WMRE concentration with respect to time. The inhibitor's corrosion rate, inhibition efficiency, and surface coverage decrease as temperature rises from 303 K to 323 K. The decrease in inhibition efficiency could be attributed to the diminishing effect of the protective coating on the mild steel coupons as temperatures rise (Emembolu, L. N. and Onukwuli, O. D., (2020)). Table 2 shows that the inhibition's efficiency decreases as temperature rises, implying that adsorbed molecules melt as the temperature of the studied solution rises. Figure 1 below illustrates the effect of corrosion rate on mild steel submerged in 1 M HCl at various temperatures 303–323K; however, due to space constraints, only two temperatures are displayed.

(a) Effects of Corrosion rates on temperature, inhibition concentration and time

Table 2 displays the rate of mild steel corrosion at various temperature and exposure durations in the absence of an inhibitor. It is evident from the table that the rate of corrosion rises with temperature for a given exposure period Ibrahim, (2022); Baskar, et al, (2022). A coating of rust forms on the sample's surface, slowing down the corrosion process, and the rate at which iron molecules dissolve in the acidic media similarly reduces as the immersion time increases Alan Miralrio and Araceli Espinoza V., (2020).

Table 2: Rate of corrosion and effectiveness of inhibition at varying WMRE concentrations.

Temp (K)	Time (hrs)	Concentration of inhibitor (mg/l)	Corrosion rate ($g/hr.m^2$)	Inhibition efficiency (IE %)	Surface Coverage (θ)
303	0	0	20.11	0	0
	2	100	6.15	51.32	0.8132
	4	200	5.54	63.56	0.8356
	6	300	5.04	75.84	0.8584
	8	400	2.50	78.96	0.8896
	10	600	1.89	85.49	0.9141
313	0	0	44.64	0	0
	2	100	15.36	75.63	0.7563
	4	200	8.98	78.73	0.7873
	6	300	7.75	80.39	0.8039
	8	400	6.90	84.91	0.8491
	10	600	4.15	87.17	0.8717
323	0	0	52.58	0	0
	2	100	20.25	66.69	0.6659
	4	200	17.23	73.40	0.7340
	6	300	14.93	78.15	0.7815
	8	400	11.40	80.07	0.8007
	10	600	9.53	88.41	0.8549

The collected reading makes it clear that temperature and corrosion rate are correlated. Significant inhibitor concentrations, however, markedly reduced the rate of corrosion. At a concentration of 600 mg/l at 323K for 10 hours, the plant extract showed a maximum IE% value of 88.41%. At a lower concentration of 100 mg/l at 303K for 2 hours, the IE% value was 51.32%. The highest level of inhibition was attained at elevated operating temperatures. The surface covering phenomenon provides an explanation for this Radha, et al, (2024). Since the plant extract covers the steel surface to prevent acidic corrosion, surface coverage is an essential part of corrosion efficiency. The plant extract's adsorbing capacity is high because it contains a lot of saponins, tanins, phenols, and other organic compounds that exist naturally and have heteroatoms like N, O, and S in their molecular structure. This aids in the flat orientation preferred adsorption of the plant extract at low concentrations. By increasing the number of

accessible inhibitor molecules, increasing the concentration to the optimal value increases inhibition efficacy and enhances surface coverage Singh, et al, (2025). Its high electron donation ability increases its ability to donate electrons to the MS during the adsorption process by guaranteeing a sufficient level of electron density at the adsorption sites Singh, et al, (2025). The presence of electron-donating groups in the plant extract, such as double bonds, hydroxyl, etc., may be related to the compound's inhibition performance. Additionally, as the inhibitor concentration rises, the corrosion rates fall (Fig 1(b)). Analysis of Fig. 1(b) below shows that CR stayed nearly constant beyond 200 mg/l. As the inhibitor concentration rises, this shows that the corrosion activity is slowing down. Additionally, it confirms the WMRE's inhibitory potentials. The adsorption-desorption equilibrium corrosion rate, or CR value at this point for each corrosive environment, is the temperature-independent point at which the rate of adsorption equals the rate at which the metal sample in the inhibited environment desorbs the WMRE

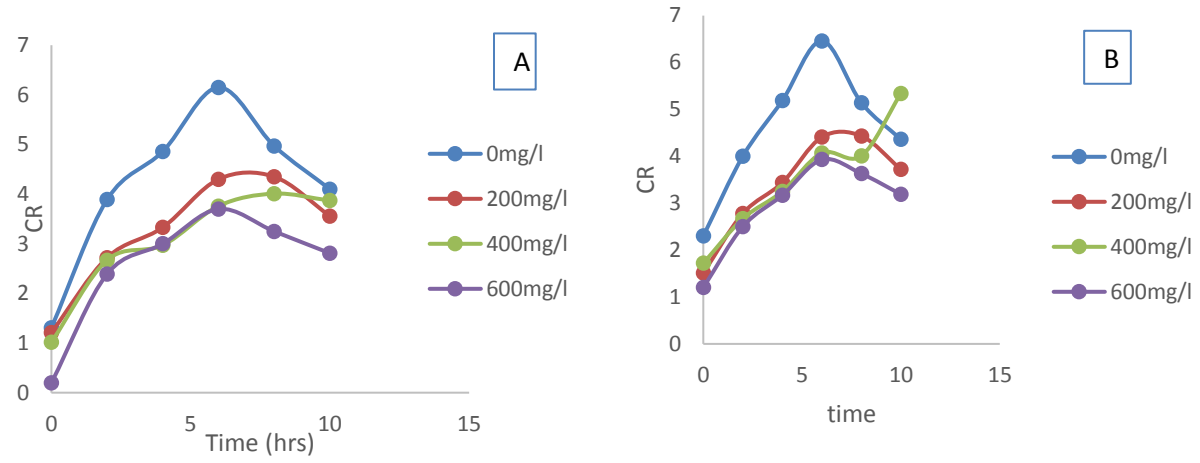

Fig 1: Plot of CR against time at (a) 303K (b) 323K

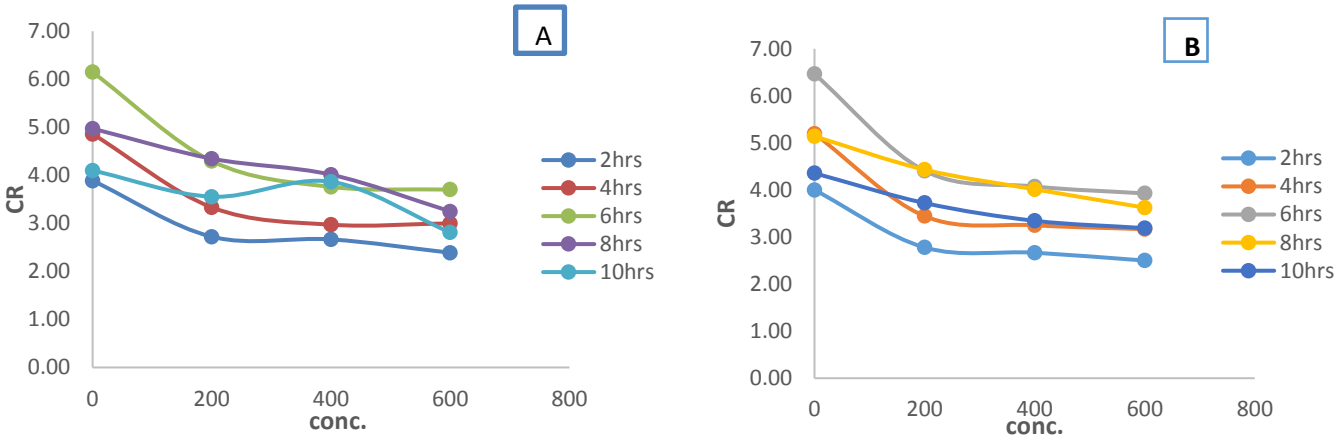

Fig. 1(b): Plots of CR against concentration at (a) 303K (b) 313K

(a) Effect of Inhibition efficiency (IE) with inhibitor concentrations and time

The correlation between inhibitor concentrations, immersion time, and inhibition efficiency (IE), as depicted in Fig. 2(a) and b), respectively, shows that inhibition effectiveness rises with increasing inhibitor concentrations and immersion time but falls with rising temperatures. This suggests that greater corrosion inhibition will arise from the

presence of more inhibitor, which in turn indicates the presence of more active components. Raising the concentration to the ideal level improves surface coverage and boosts inhibition efficacy by expanding the pool of available inhibitor molecules Singh, et al, (2025). By ensuring a sufficient level of electron density at the adsorption sites, its strong electron donation ability enhances its capacity to donate electrons to the MS during the adsorption process Singh, et al, (2025);. The compound's ability to inhibit may be correlated with the presence of electron-donating groups in the plant extract, such as hydroxyl, double bonds, etc.

3.3 Instrumental Analysis

3.3.1 FTIR Analysis

FTIR was used to investigate the functional groups in WMRE, and the results are shown in Fig. 3 below. The FTIR spectrum's transmissibility through the WMRE at wavelengths ranging from 700 cm-1 to 4000 cm-1 are displayed in the spectra below. The transmissibility's at 1500cm-1-1700cm-1 and 3000cm-1-3500cm-1 show a discernible decline. These ranges correspond to the carboxyl group's carbonyl (C=O) group stretching vibrations and the amino group's amine (N-H) group stretching vibrations, respectively. Thus, the plant extract was characterized using infrared spectroscopy. There was a shift in the spectra of the extract when mild - steel was immersed in 1M HCl. This indicates that the extract and the carbon steel substrate interacted in a way that caused inhibition. The alterations in the spectra are believed to be caused by the extracts' interaction with mild steel through their functional groups. Given this, it is verified that the functional group formed a Fe^{2+} extract complex with the Fe^{2+} produced on the metal surface, which helped to block the metal sample Odewunmi, et al. in 2015.

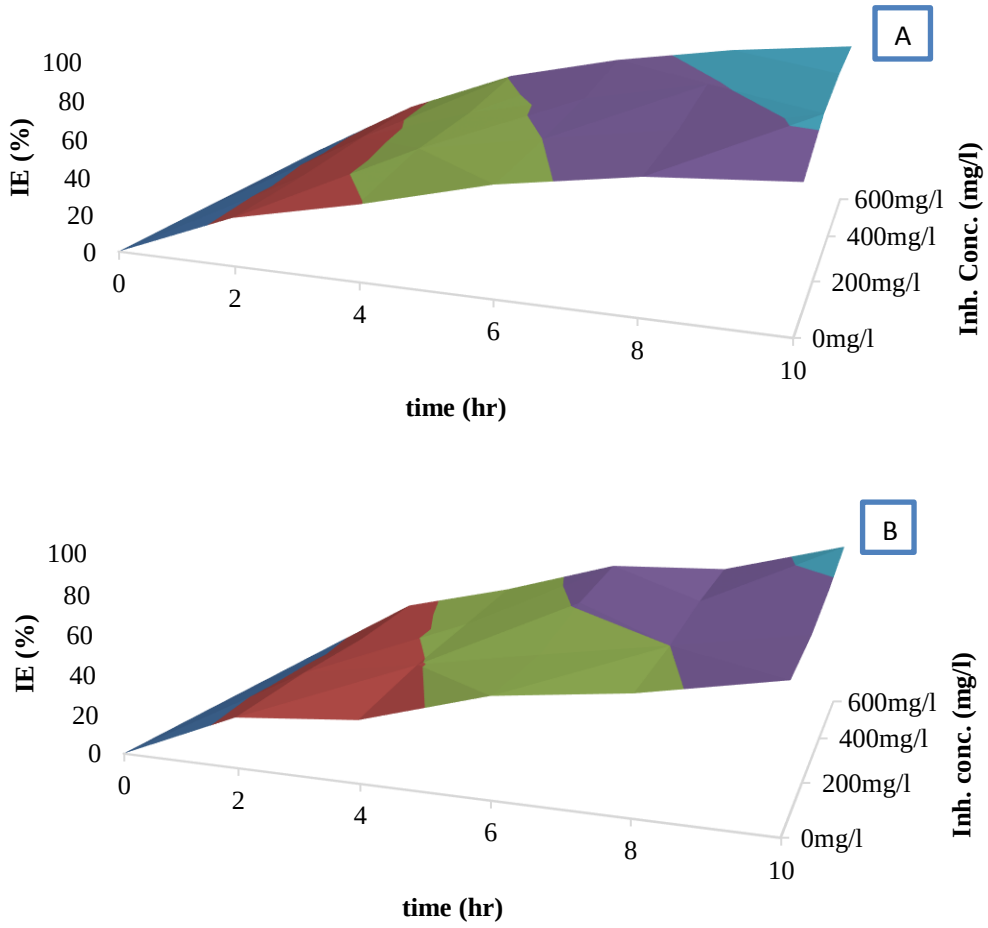

Fig 2: Relationship between IE (%) with immersion time and inhibitor concentrations at (a) 303K (b) 323K

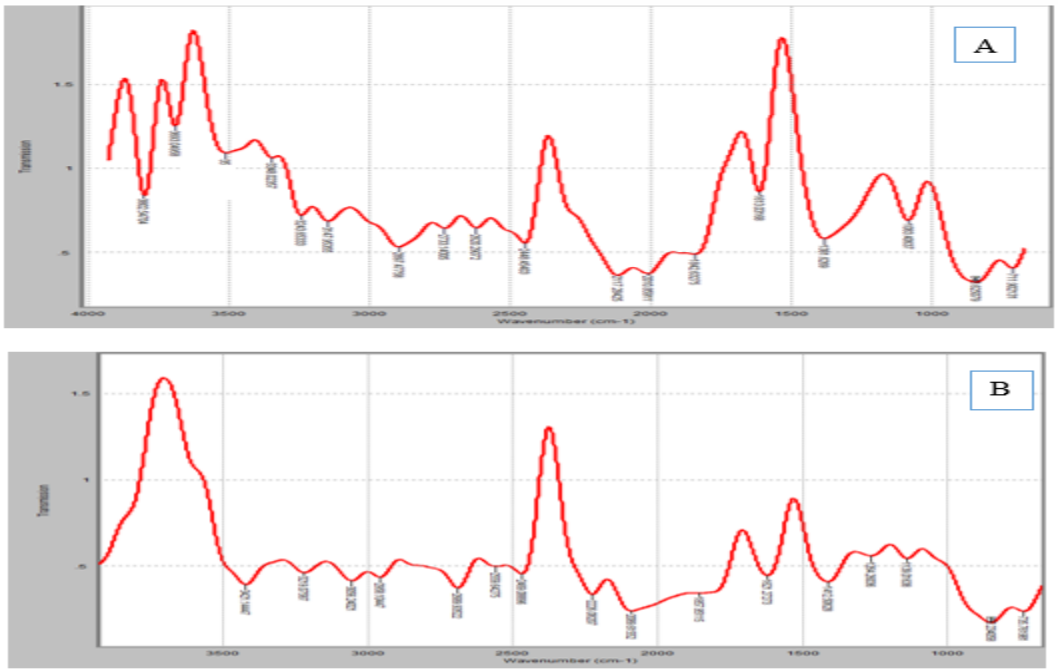

Fig 3: WMRE's FTIR spectra (a) prior to and (b) following the experiment.

3.3.2 SEM/EDX Analysis

The surface morphology of mild steel in the absence and present of 1 M HCl for 12 hours at different temperatures were examined using scanning electron microscopy (SEM) and energy dispersive spectroscopy (EDX). The inferrence drawn were shown on Fig 4 and Fig 5 respectively. Regardless of whether it is prevented or not, the SEM pictures demonstrate that mild steel coupon corrosion in an acidic environment is not uniform. For example, after polishing with various grades of emery cloth, the mild steel surface in Fig. 4(a) above appeared smooth to the unaided eye. The mild steel coupon in uninhibited 1M HCl was significantly corroded, with some pits and cracks, as shown once more in Fig. 4(b).

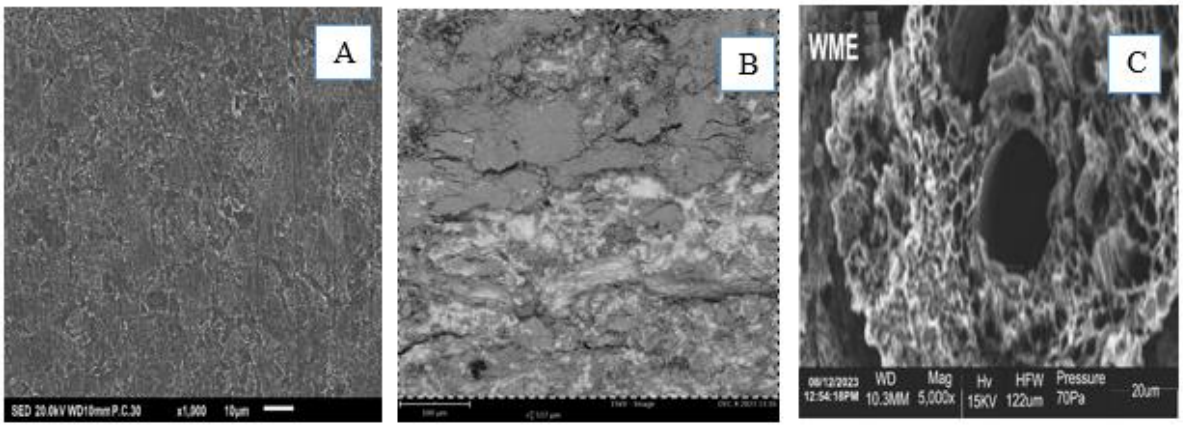

Fig 4: A mild-steel coupon SEM micrograph: (a) a polished (b) in 1 M HCl only (c) in 1M HCl with WMRE

The WMRE, however, is shielded by a "cloud-like" layer in Fig. 4(c) that prevents the actual metallic material from corroding as pits or fractures in the suppressed 1 M HCl environment Nikitia, et al, (2023). This can be attributed to

the adsorption of WMRE's on the metal surface, which would limit the possibility of a metal-oxygen or metal-acid reaction that leads to corrosion because of its (WMRE) anti-oxidant components. Again, it is anticipated that if the sample is left in the inhibited environment for a longer period, the WMRE will cover the entire surface of the metallic sample, preventing further corrosion. Therefore, the WMRE protects the mild steel surfaces from both the oxygen-driven corrosion and the acid-driven corrosion. The elements present on the metal surface before and after immersion to the inhibitor solution were identified by Energy-Dispersive Spectroscopy (EDX) as presented in Fig 5.

The elemental distribution and EDX spectra for a mild steel sample in a 1M HCl solution are displayed in Fig. 5(a) as Carbon 0.9, Oxygen 31.0, and Fe 68.1, respectively. However, as shown in Fig. 5(b), the EDX spectrum reveals additional peaks of 0.5% each for nitrogen and chlorine in the presence of 1M HCl including WMRE. These peaks were suggestive of adsorbed extract species. Further validating the adsorption of WMRE on the metal surface and providing good corrosion protection, the weight and atom percentages of Fe in the mild steel surface increased noticeably from 68.1 to 92.5% and from 37.8 to 75.5%, respectively. It is equally evident that carbon exhibits an increasing tendency with iron.

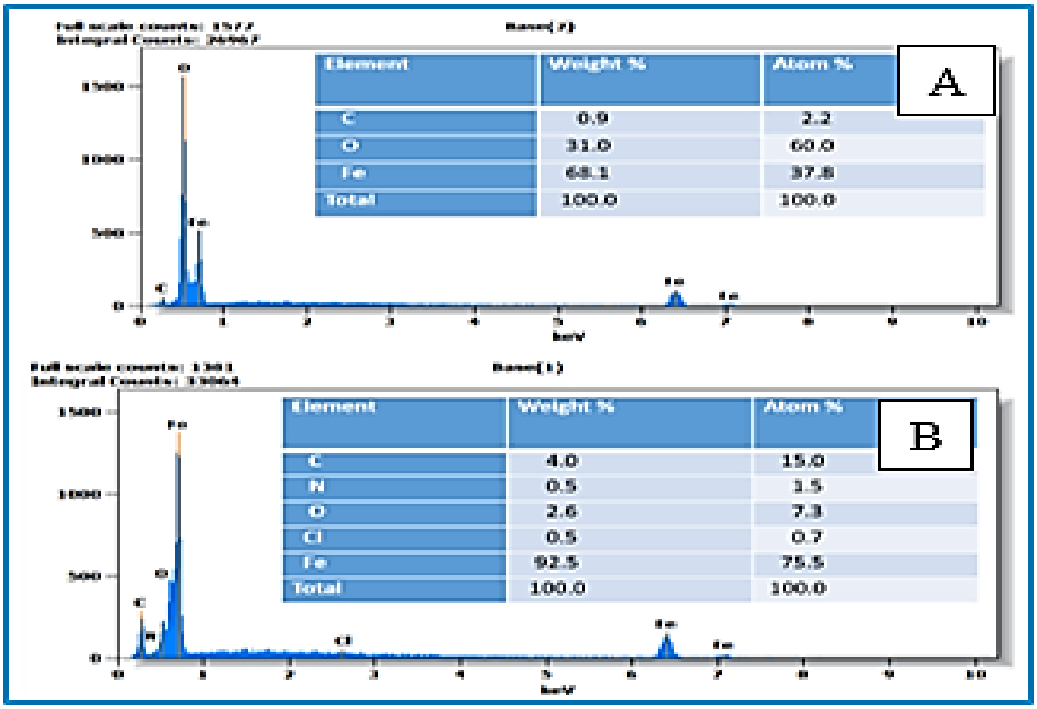

Fig 5: Mild -steel micrograph EDX plots in: (a) 1 M HCl only (b) 1 M HCl with WMRE

3.4 Thermodynamics and Adsorption isotherms

Information about the adsorption of inhibitors on metal surfaces is provided via adsorption isotherms. Therefore, using various adsorption isotherm models such as Frumkin (Eq. 4), Langmuir (Eq. 5), and Temkin (Eq. 6) below, the behavior of inhibitors on the metal surface and the relationship between the surface coverage (θ) and the inhibitor concentrations (C_{inh}) were assessed.

$$log\left[C\left(\frac{\theta}{1-\theta}\right)\right] = 2.303logK + 2\alpha\theta \quad (4)$$

$$\frac{K}{\theta} = \frac{1}{K_{ads}} + C \quad (5)$$

$$\theta = \frac{2.303logK}{2a} - \frac{2.303logC}{2a} \quad (6)$$

where "a" is the attractive parameter, "C" is the inhibitor concentration, "α" is the lateral interaction term that describes the characteristics of the adsorbed layer, and "K_{ads}" is the adsorption equilibrium.

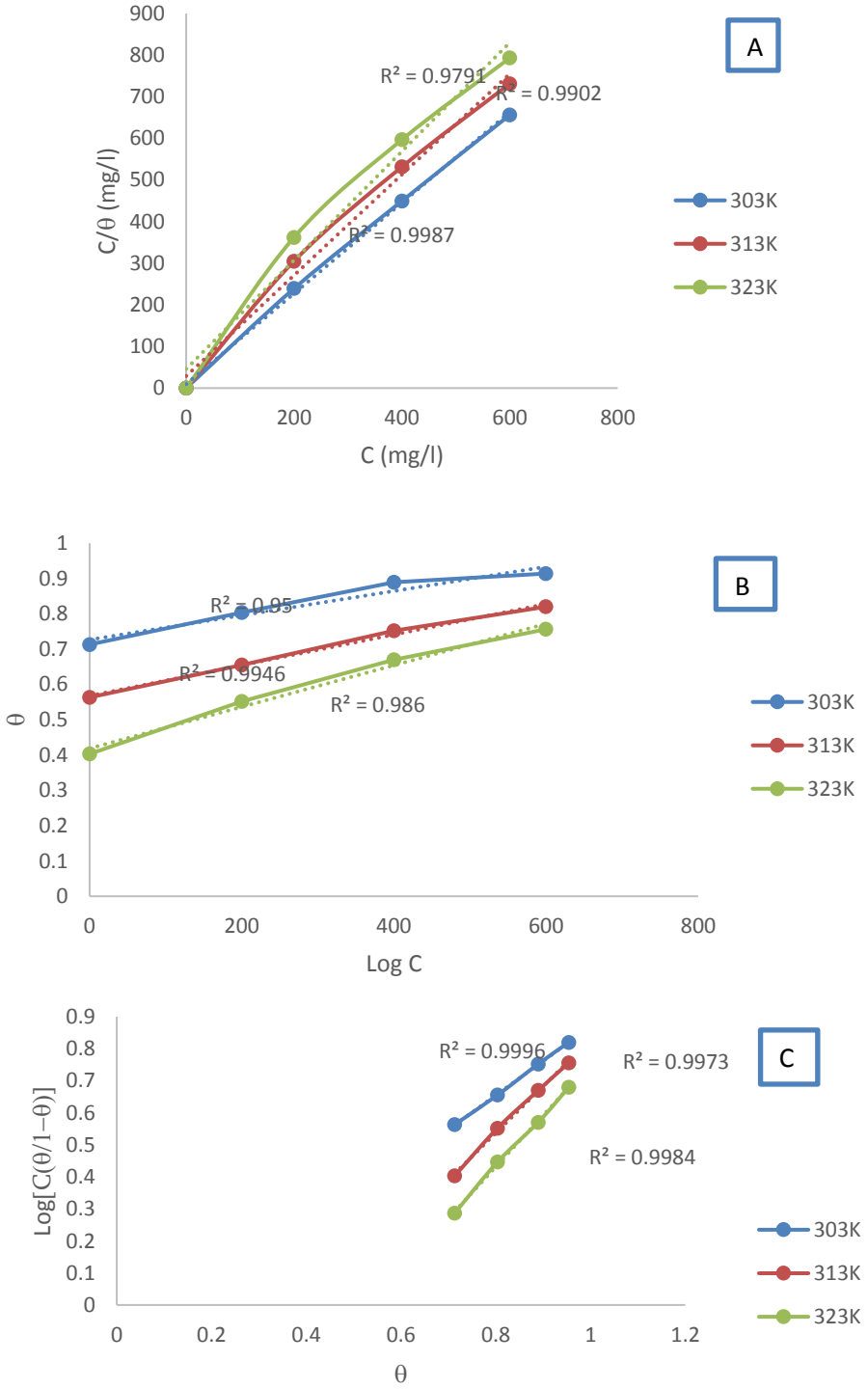

Fig. 6: WMRE adsorption isotherms on the surface of mild steel: (a) Langmuir (b) Temkin (c) Frumkin.

Correlation coefficient (R^2) values at three distinct temperatures were used to evaluate the adsorption isotherms' fitness. For Langmuir, Temkin, and Frumkin, the average correlation coefficient data were 0.9893, 0.9769, and 0.9983, respectively. The resulting result indicates that the Frumkin, Langmuir, and Temkin isotherm models fit the adsorption isotherm modeling the best, in descending order. The evaluation of the three isotherm results is shown in Table 3 below. The greater the K_{ads} value, the more strongly the inhibitor binds to the metal surface. Equation 7 links K_{ads} values to the heat of adsorption (Ezeugo, 2018; Onukwuli et al., 2020). The (K_{ads}) known as adsorption equilibrium constant can be connected with the standard free enthalpy through the following relationship:

$$K_{ads} = \frac{1}{55.5} exp\left(-\frac{G_{ads}}{RT}\right) \quad (7)$$

55.5 (mol/l) = the concentration of water in the solution, R is the gas constant in (J/mol/K).

Table 3: Adsorption coefficients based on Frumkin.

Isotherm model	Temp. K	R^2	K_{ads}	ΔG_{ads} (KJ/mol)	ΔH_{ads} (KJ/mol)	ΔS_{ads} (J/mol.K)
Frumkin	303	0.9996	0.082	-4.03		
	313	0.9973	0.079	-3.43	-40.10	-5.20
	323	0.9984	0.075	-3.67		

The average value of ΔG_{ads} for the three temperatures on Table 3 is -3.71 kJ/mol. The obtained ΔG_{ads} values indicates physical adsorption as can be seen in Table 3. Also, the standard entropy and enthalpy of the process was determined by applying Vant Hoff equation; (Eq. 8) and 9 respectively and plotted in Fig. 7 accordingly.
It is equally understandable that adsorption processes utilizes enormous energy in form of heat which results in lowering the entropy of the process as well.

$$\ln K = -\frac{\Delta H_{ads}}{RT} + Constant \quad (8)$$

$$\Delta G_{ads} = \Delta H_{ads} - T\Delta S_{ads} \quad (9)$$

Table 1 shows that corrosion rate increases as the temperature increases. Thus the effect of temperature on the corrosion process can assessed and evaluated using Arrhenius equation (Eq. 10) and transition state equation (Eq.11) see Fig 8. Table 4 presents the kinetics parameters namely activation energy (Ea), frequency factors (A), enthalpy of activation (ΔH), and entropy of activation (ΔS) were cacalculated from the slopes of and intercepts of Eqs. 10 and 11 respectively [Emembolu, and Onukwuli, (2020); Eliaz, N. (2019)].

$$CR = Aexp\left(-\frac{E_a}{RT}\right) \quad (10)$$

$$CR = \left(\frac{RT}{Nh}\right) exp\left(\frac{\Delta S}{R}\right) exp\left(-\frac{\Delta H}{RT}\right) \quad (11)$$

Where h, and N is Plank's constant, and Avogadro's number, respectively.

Table 4: Arrhenius and transition-state parameters for mild-steel in 1 M HCl.

C_{inh} (mg/l)	E_a (KJ/mol)	ΔH (KJ/mol)	-ΔS (J/molK)
Blank	25.10	20.25	144.20
200	30.42	41.41	30.78
400	34.12	52.5	50.13
600	40.15	75.33	82.12

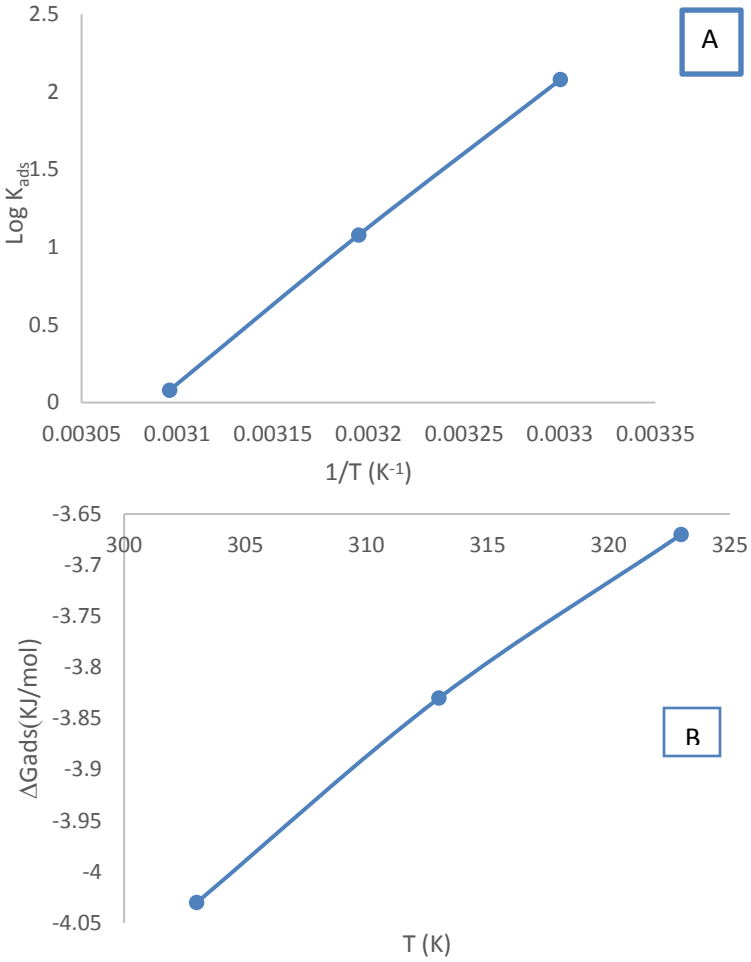

Fig. 7: (a) Vant Hoff equation (b) Heat of adsorption.

It is commonly acknowledged that the activation energy (Ea) is the bare minimum of energy required for reactants to start a chemical reaction. Iroha, and Nnanna, (2019); Wang, et al, (2019). One can see from Table 4 above that the reactants (parameters) are truly impacted by an increase in the inhibitor concentration. As a result, the value of Ea obtained with the inhibitor was higher than without it, indicating that the MS surface developed a WMRE layer, raising the energy barrier. The physical adsorption mechanism is responsible for this increase in Ea. Once more, the experiences of Ea and.ΔHads are similar. The presence of an association step instead of a dissociation phase during the transition from reactant to activated complex is indicated by the negative values for ΔSads, which imply an activated complex [Eliaz, N. (2019); Onukwuli, et al, 2020; Tsoeunyane, et al, 2019; Olorunmaiye, et al, (2019)].

4.0. Conclusion

It has been investigated how well WMRE inhibits MS corrosion in an acidic media at high temperatures and after extended time exposure. The experimental data fit to Frumkin-Langmuir isotherm models further supported the extract's adsorption via a physicochemical mechanism. The effectiveness of the inhibitor was investigated using the weight loss approach. High inhibitor concentrations and low operating temperatures resulted in a maximum efficiency of 88.41% over a 12-hour period. The SEM/EDX data showed how effective the inhibitor was at preventing corrosion and mild steel surface degradation. While FTIR determined the extract's organic components, GC-FID showed the amount of phytochemicals. With a similar amount of inhibition and no harmful ingredients, the WMRE plant extract is less costly and more environmentally friendly than conventional synthetic corrosion inhibitors.

References

Amine, et al, 2023, Corrosion inhibition effect of Raphia palm extract on mild steel in citric acid. International journal of material science, 4.

Anaele, & Ipeghan,, 2018, Study of Corrosion inhibition of pineapple peels extracts on mild steel in 1M HCl. Journal of Scientific and Engineering research, 5.

Askeland, and Phule, 2016, Carbon steel, Material science and Engineering, 9th ed.

Baskar, et al, 2022 Use of Trochodendron Aralioides Extract as Green Corrosion Inhibitor for Mild Steel in 1M HCl Solutions. Processes, 10, 1480. https://doi.org/10.3390/pr10081480

Bramantyo, et al, 2024. Photocatalysis on Selective Hydroxylation of Benzene to Phenol. Solar Light-to-Hydrogenated Organic Conversion. doi:10.1007/978-981-99-8114-4_5

Eliaz, 2019 Corrosion of Metallic Biomaterials. *Materials, 12*(3), 400-407. doi:: 10.3390/ma12030407

Emembolu and Igwegbe, 2022, Investigation of Temperature Correlations on Corrosion Inhibition of Carbon Steel in Acid Media by Flower Extract, European Journal of Engineering and Applied Sciences, 5(1), 29-36. http://dx.doi.org/ 10.55581/ejeas.1127813

Emembolu, and Onukwuli, 2020, Inhibitive effect and adsorption study of *Chromolena odorata* and *Aspilia africana* as corrosion inhibition of zinc in 1 M H_2SO_4 solution, Journal of Engineering and Applied Sciences, 16(1), 108-116

Harsimran, et al, 2021. Overview of corrosion and its control. Proceedings of Engineering Sciences, 13-24. https://doi.org /10.1007/s42250-022-00531-0

Ibrahim, 2022, Experimental and Theoretical Evaluation Of Corrosion Inhibition of Honeycomb Propolis Extract On Mild Steel In Acidic Media, J. Mater. Environ. Sci., 13(5), 576-598

Iroha and Nnanna, 2019, Electrochemical and Adsorption Study of the anticorrosion behavior of Cefepime on Pipeline steel surface in acidic Solution, J. Mater. Environ. Sci. 10(10): 898-908

Joseph Ezeugo, 2018, Optimization of corrosion inhibition of *Picralima nitida* seed extracts as a green corrosion inhibitor for zinc in 0.5 M H2SO4, International Journal of Chemical Studies. 6(4): 2080-2088

Jun, et al, 2018, impacts of quality corrosion of cast ironpipe for water distribution and proposed source water switch strategy. Water research, 129, doi: https://doi.org/10.1016/j.watres/2017.10.065

Kadhim, & Albdiry, 2017. A critical review on corrosion and its prevention in the oilfield equipment. *Journal of Petroleum Research and Study*, 162-189.

Lasisi, et al 2023, the inhibitive performance of WRE on corrosion behavior of mild steel in 0.5 M H2S04. Achievers journal of scientific research, 4.

Mohamed A. O., 2022, Optimization of mild steel corrosion inhibition by water hyacinth and common reed extracts in acid media using factorial experimental design, Green Chemistry Letters and Reviews, 15(1), 216-232, DOI: 10.1080/17518253.2022.2032844

Mohammad, et al, 2024. Screening of different extraction methods for maximum production of total flavonoids, tannins, and antioxidants from Centella asiatica. *Food Research*, 44-51, doi:10.26656/fr.2017.8(1).057

Nikitia, et al, 2023. Chemo- and regio-selective enzymatic lipophilisation of rutin, and physicochemical and antioxidant properties of rutin ester derivatives. *RSC Advances*.

Nnanna, 2018. Phytochemical Composition, Anti-Nutrient Properties And Antioxidant Potentials Of Hibiscus Sabdariffa Seeds. *West African Society Of Toxicology International Conference.* Abuja.

Odewunmi, et al, 2015, Watermelon wasteproducts as green corrosion inhibitors for mild steel in HCl solution. *Journal of Environmental Chemical Engineering*, 286-296.

Okeoma, et al, 2022, Corrosion inhibition potential of Elaesis Gineensis leave extract on X70 carbon steel using weight loss method. International conference of the Nigeria Institution of Mechanical Engineers, Nigeria.

Olivia, et al, 2023, Corrosion inhibition of mild steel bars by biosurfactants produced by *Penicillium citrinum*, IOP Conference series: Earth and environment science. doi.org/10.1088/1755-1315/1135/1/012057

Olorunmaiye, et al, 2019, Proximate and Phytochemical Composition of African Mahogany (*Afzelia africana)* seed and African mesquite (*Prosopis africana)* pod, J. Appl. Sci. Environ. Manage. 23(2): 249–252

Onukwuli, et al, 2020,Optimum prediction for inhibition efficiency of *Sapium ellipticum* leaf extract as corrosion inhibitor of aluminum alloy (aa3003) in hydrochloric acid solution using electrochemical impedance spectroscopy and response surface, methodology, Bull. Chem. Soc. Ethiop. 34(1): 175-191, DOI: https://dx.doi.org/10.4314/bcse.v34i1.17

Onyenanu, et al, 2022, Corrosion Inhibition potentials of *A. mossambicensis* and *E. sonchifolia* Leaves' Extracts on Aluminuium in Alkaline Media: Insights from Gravimetric and Electrochemical Studies, Chemistry Africa**,** https://doi.org /10.1007/s42250-022-00531-0

Priyotomo, et al, 2022, Corrosion inhibition of carbon steel in sulfuric acid using Cymbopogon citratus as a green Corrosion inhibitor. Corrosion science and technology. Doi:10.14773/cst.2022.21.6.423

Tsoeunyane, et al, 2019, Corrosion Inhibition of Mild Steel by Poly (butylene succinate)-L-histidine Extended with 1, 6-diisocynatohexane Polymer Composite in 1 M HCl, International Journal of Corrosion. Article ID 7406409, https://doi.org/10.1155/2019/7406409

Wang,et al, 2019, Solanum lasiocarpum L. Extract as Green Corrosion Inhibitor for A3 Steel in 1 M HCl Solution, Int. J. Electrochem. Sci. 14: 1178 – 1196, DOI: 10.20964/2019.02.06

Emembolu, etal, 2024, Corrosion Inhibition Performance of Brachystegia eurycoma Leaf Extract on Mild Steel in Acid Media, Journal of Engineering Research and Reports, 26(6), 83-102. DOI: 10.9734/JERR/2024/v26i61164

Ali, et al, 2022, Plant extracts as sustainable and green corrosion inhibitors for protection of ferrous metals in corrosive media: A mini review, Corrosion Communications, 5, 25-38, https://doi.org/10.1016/j.corcom.2022.03.002.

Bhoomika, et al, 2024, Plant extracts as green corrosion inhibitors for different kinds of steel: A review, Heliyon, 10(14), https://doi.org/10.1016/j.heliyon.2024.e33748.

Norbaayah, et al, 2021**,** A Review on Plants and Biomass Wastes as Organic Green Corrosion Inhibitors for Mild Steel in Acidic Environment, *Metals*, *11*(7), 1062; https://doi.org/10.3390/met11071062

Barboza, et al, 2024, *Justicia brandegeeana* as a green corrosion inhibitor for carbon steel in sulfuric acid. *Green Chemistry Letters and Reviews*, *17*(1). https://doi.org/10.1080/17518253.2024.2320254

Alan Miralrio and Araceli Espinoza V., 2020, Plant Extracts as Green Corrosion Inhibitors for Different Metal Surfaces and Corrosive Media: A Review**,** *Processes*, *8*(8), 942; https://doi.org/10.3390/pr8080942

Radha, et al, 2024, Experimental study on corrosion inhibition of mild steel using *Mukia maderaspatana* leaves extract as green inhibitor, Surf. Sci. Tech. **2**(27). https://doi.org/10.1007/s44251-024-00056-3

Singh, et al, 2025, A sustainable and green method for controlling acidic corrosion on mild steel using leaves of Araucaria heterophylla. Sci Rep, 15(1), doi: 10.1038/s41598-025-86352-w.

Emembolu, et al, 2021, Electrochemical and statistical study of the inhibition effect of T. conophorum leaf extract on aluminum corrosion in acidic medium, Safety in Extreme Environments. https://doi.org/10.1007/s42797-021-00040-2